# Airborne Collision Scenario Flight Tests: Impact of Angle Measurement Errors on Reactive Vision-based Avoidance Control

Troy S. Bruggemann [1], Luis Mejias [1]

[1] *Australian Research Centre for Aerospace Automation, 22-24 Boronia Road Brisbane Airport, Queensland, 4007*

**Abstract**

The future emergence of many types of airborne vehicles and unpiloted aircraft in the national airspace means collision avoidance is of primary concern in an uncooperative airspace environment. The ability to replicate a pilot's see and avoid capability using cameras coupled with vision-based avoidance control is an important part of an overall collision avoidance strategy. But unfortunately without range collision avoidance has no direct way to guarantee a level of safety.

Collision scenario flight tests with two aircraft and a monocular camera threat detection and tracking system were used to study the accuracy of image-derived angle measurements. The effect of image-derived angle errors on reactive vision-based avoidance performance was then studied by simulation. The results show that whilst large angle measurement errors can significantly affect minimum ranging characteristics across a variety of initial conditions and closing speeds, the minimum range is always bounded and a collision never occurs.

**Keywords:** collision avoidance, vision-based control.

## Introduction

The future emergence of many different types of airborne vehicles and unpiloted aircraft in the national airspace means collision avoidance is of primary concern. Many of the currently used collision avoidance approaches rely upon continuous datalinks (such as ADS-B or TCAS) or assume line of sight range to a threat is available [3,8]. Alternatively, non-cooperative and passive systems relying upon vision-based detection and tracking of collision threats (also known as see and avoid) could be suitable for aircraft that do not use TCAS or ADS-B [5]. A number of recent see and avoid approaches have resulted from machine vision and robotics research [2, 5, 6, 7, 10, 11]. A passive and reactive automatic collision avoidance control system utilizing vision is highly dependent upon the accuracy of the measurements of relative bearing and elevation to the threat [2]. Angle measurements to the threat are made in the image plane by a camera mounted to the aircraft body, and typically do not reflect the true angles in a navigation (or world) frame where collision avoidance occurs [4]. Thus, there is concern that mismatch between the estimates of angles to the threat in the image plane, and the true angles to the threat in the world frame can lead to ineffective (and even unsafe) collision avoidance control.

The purpose of this paper is to study the effect of angle measurement errors on vision-based collision avoidance performance. A series of collision scenario flight tests (involving two

Cessna aircraft) with a monocular vision system was used to determine the accuracy of image-derived bearing and elevation estimates to a threat [5]. Following this, the effect of image-derived angle errors on reactive avoidance performance was studied by simulation of collision avoidance with a closed-loop reactive vision-based collision avoidance control system.

## Reactive Vision-based Collision Avoidance Control

Fig. 1 illustrates a typical collision avoidance control architecture utilizing vision-based control. The design consists of a vision detect and sense system [5] which detects and tracks potential threats and collision avoidance control which issues commands to the aircraft autopilot to command a change of course, to maintain separation from the threat [2,11]. The feedback path from the aircraft to the vision system highlights a typical closed-loop design. Clearly, the collision avoidance control is very much dependent upon the vision detect and sense system, both for detection and for continuous tracking of the threat. A key challenge is that there is assumed no knowledge of the threat aircraft's state or range, except what information can be derived passively from the image (e.g. initial range may be estimated by observing successive image frames over time [11]).

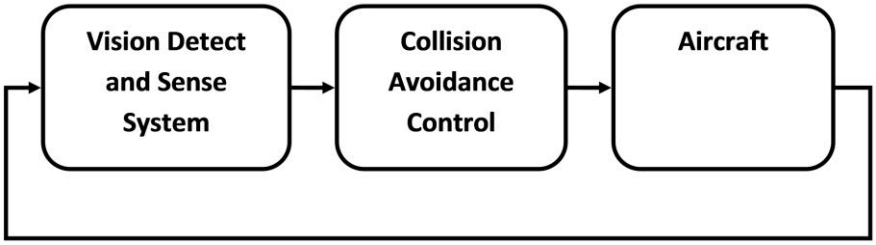


*Fig. 1: Collision Avoidance Control Architecture.*

### Aircraft Dynamics

In a North, East, Up navigation frame, the aircraft's translational motion can be described by [1],

$$\begin{aligned} \dot{x} &= V \cos \chi \cos \gamma \\ \dot{y} &= V \sin \chi \cos \gamma \\ \dot{z} &= V \sin \gamma \end{aligned} \qquad (1)$$

where *x,y,z* is aircraft position, *V* is magnitude of aircraft velocity vector with respect to Earth, $\chi$ is the track angle from North and $\gamma$ is flight path angle with respect to the ground. A collision may occur if $\Delta\dot{\chi} = 0$ and $\Delta\dot{\gamma} = 0$ where $\Delta\dot{\chi}$ and $\Delta\dot{\gamma}$ are the relative track and relative flight path angles to the threat.

In flight, track angle $\chi$ is related to heading angle $\psi$ by $\chi = \psi + \beta + \chi_w$ where $\beta$ is sideslip angle and $\chi_w$ is drift angle due to wind [4]. The flight path angle $\gamma_g$ is related to pitch angle $\theta$ by $\gamma_g = \theta - \alpha - \gamma_w$ where $\alpha$ is angle of attack and $\gamma_w$ is the angle between airspeed and Earth speed vectors due to wind [4].

Manoeuvring the aircraft horizontally or vertically to maintain safe spatial separation from a threat can be accomplished by adjusting track angle $\chi$ and (or) flight path angle $\gamma$ through a change of body-frame roll, pitch and yaw attitude angles $\Theta = (\phi, \theta, \psi)$ [1, 9].

**Camera-derived Measurement of Relative Angles to a Threat**

In vision-based control the image-derived relative bearing $\Delta\psi^i$ and relative elevation $\Delta\theta^i$ angles to the threat can be used to command a change of $\Theta$ to maintain separation. Assuming a forward facing camera fixed to the body of the aircraft, the image-derived relative angles to the threat at discrete time *k* can be estimated as [7],

$$\begin{aligned} \Delta\psi_k^i &= \tan^{-1}\left(\frac{u_k^i - 0.5w}{f}\right) \\ \Delta\theta_k^i &= \tan^{-1}\left(\frac{v_k^i - 0.5h}{f}\right) \end{aligned} \qquad (2)$$

where $P_k^i = (u_k^i, v_k^i)$ is the pixel position of a threat (or intruder) aircraft in the image frame, *f* is camera focal length, *w* and *h* is the width and height of the image. We use a standard projective model and assume distortion errors in the model have been corrected. $P_k^i$ can be estimated using a morphological-HMM filter [5].

However, $\Delta\psi^i$ and $\Delta\theta^i$ are estimates of body-frame angles to the threat, which provide an inaccurate estimate of the true relative bearing angle to the threat due to unaccounted drift and attack angles. Using $\Delta\psi^i$ and $\Delta\theta^i$ directly in a closed-loop feedback controller could result in under or overestimation of the control action required to avoid the threat.

By simple geometry [4] the body frame estimates from the image ($\Delta\psi^i$ and $\Delta\theta^i$) can be transformed into the navigation frame relative track $\Delta\chi^i$ and relative flight path $\Delta\gamma^i$ angles by,

$$\begin{aligned} \Delta\chi_k^i &= \psi_k - \chi_k + \Delta\psi_k^i \\ \Delta\gamma_k^i &= \gamma_k - \theta_k + \Delta\theta_k^i \end{aligned} \qquad (3)$$

where $\chi_k, \psi_k, \theta_k, \gamma_k$ can be measured from an onboard navigation system.

**Lateral Vision-based Reactive Collision Avoidance Control**

A lateral vision-based reactive avoidance controller based upon the principle of adjusting aircraft course by keeping a threat at a constant relative bearing angle (or line of sight) angle was described in [11, 12]. This control approach is illustrated by Fig. 2 steps *(1), (2)* and *(3),* which shows an aircraft *A* avoiding threat aircraft *B* by following a spiral arc by maintaining a constant relative bearing angle $\overline{\alpha}$ to aircraft B. If no avoidance manoeuvre occurred, aircraft *A* and *B* would collide at point *C*.

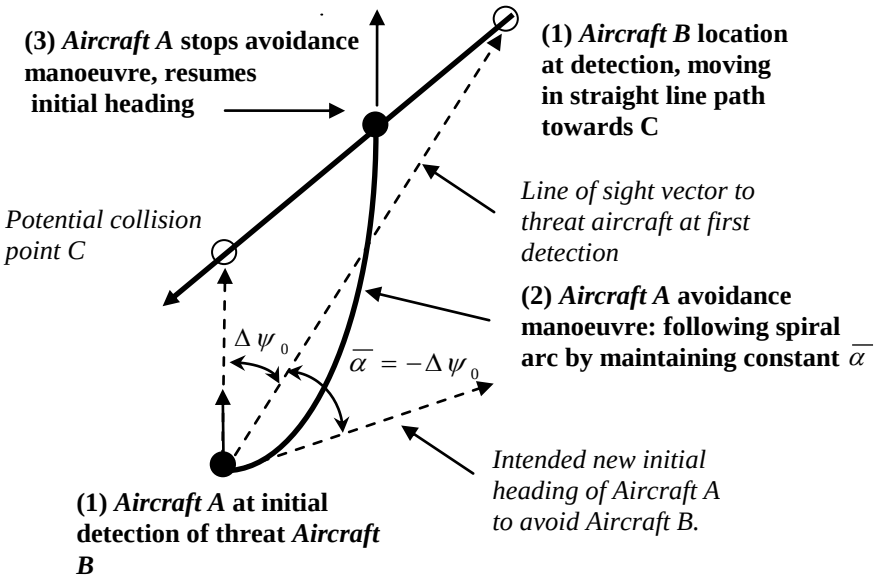


*Fig. 2: Illustration of vision-based reactive collision avoidance.*

Let $\bar{\alpha}$ be a desired constant relative bearing angle to the threat, where $\bar{\alpha} < 0.5F$ and $F$ is the camera's field of view. A vision-based controller can command a change of heading $\Delta\psi_c^i$ to change the aircraft course angle $\Delta\chi_k^i$ by:

$$\Delta\psi_c^i = f(\Delta\psi_k^i - \bar{\alpha}), \qquad (4)$$

$$\Delta\chi_k = f(\Delta\psi_c^i). \qquad (5)$$

Maintaining a constant relative bearing angle $\bar{\alpha}$ has the unique property that the flight path will approximate a spiral arc, and is inspired by the way moth insects track to a light source [13]. In vision-based control this corresponds to keeping a tracked threat at a fixed position within an image.

Collision avoidance performance is dependent upon appropriate choice of $\bar{\alpha}$. A simple control policy is as follows; under the assumption that the threat aircraft's flight path will follow an approximately straight line (for a short-duration reactive avoidance scenario), the controller will adjust the aircraft's course angle such that the desired constant relative bearing angle $\bar{\alpha}$ is the opposite of the relative bearing angle to the threat at first detection:

$$\bar{\alpha} = -\Delta\psi_0. \qquad (6)$$

In the image plane this corresponds to moving the threat from one half of the image to the other. That is, moving the threat from the left to the right of the image plane corresponds to a left turn in the navigation frame, and vice versa. This policy also prevents the aircraft from crossing in front of the oncoming intruder's path (with a straight line threat aircraft flight path assumption). There is a special situation when $\Delta\psi_0^i = 0$, then $\bar{\alpha} = \mathrm{K}$ where $\mathrm{K} < 0.5F, K \neq 0$ is a chosen constant.

Collision avoidance control continues until a stopping condition is reached (e.g. when the threat aircraft leaves the camera field of view or when the ownship aircraft arrives at its

original heading). A stopping condition is necessary to prevent the controller from chasing the threat aircraft [11].

Because this is purely a vision-based approach with no closed loop measurement of range to the threat, there is no direct way to guarantee a desired minimum range to the threat (but minimum range may be influenced indirectly via choice of $\bar{\alpha}$). Hence, in this paper a simulation study of the effect which angular measurement errors have on minimum range is given, for the control policy just described.

## Test Case 1: Accuracy of Image-derived Angles in Collision Scenario Flight Tests

Five collision scenario flights between two Cessna 172 aircraft in a tail-chase scenario were conducted in South-East Queensland, Australia. The chasing aircraft (ownship) was equipped with a monocular camera threat detect and tracking system which was mounted and aligned on the wing strut as shown by Fig. 3 [5]. The laboratory-measured angle accuracy of the camera system was < 1 deg and field of view was 20 deg. Both aircraft were equipped by onboard survey-grade navigation systems for the purpose of calculating the true relative angles in the navigation frame (within 0.5 deg accuracy).

The two aircraft flew behind each other in a tail chase scenario (for safety both aircraft were separated vertically) and the closing speed was approximately 20 m/s (see Fig. 4). During flight the intruder aircraft was continuously tracked when detected in range (at about 1919 m), and estimates of bearing and elevation to the intruder were derived from images at a rate of 15 Hz (Fig. 5).


*Fig. 3: Camera pod mounted on wing strut of Cessna 172 ownship (chase aircraft).*

Fig. 6-7 shows the image-derived and navigation system-derived angle measurements for one of the five flight tests in which the intruder was tracked over a period of 1.5 minutes. Dot points on the figures indicate when tracking data was available. We note that there were some periods when tracking was lost (such as between 21-25 seconds and between 65-75 seconds). Sudden aircraft motion due to turbulence caused image jitter resulting in the camera system to lose tracking momentarily. Also, as the range to the threat decreased, the motion of the threat in the image became larger which may have also contributed to a loss of tracking. These issues were discussed in [5] and are an ongoing area of research.

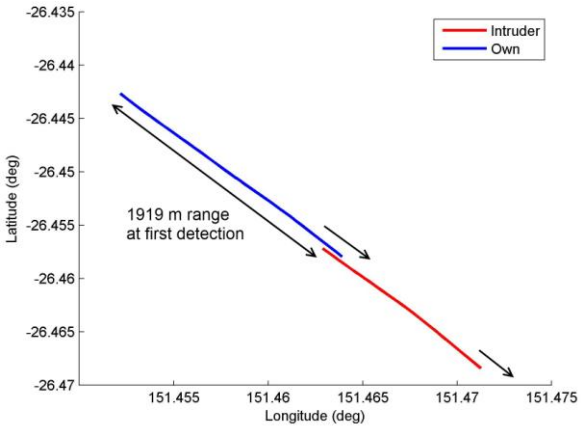


*Fig. 4: Aircraft ground tracks for tail chase flight test. The intruder was first detected at 1919 m range.*

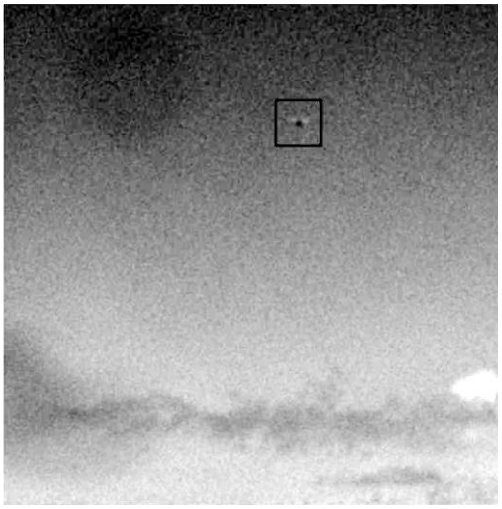

*Fig. 5: Intruder (chased) aircraft tracked in image as highlighted by black box.*

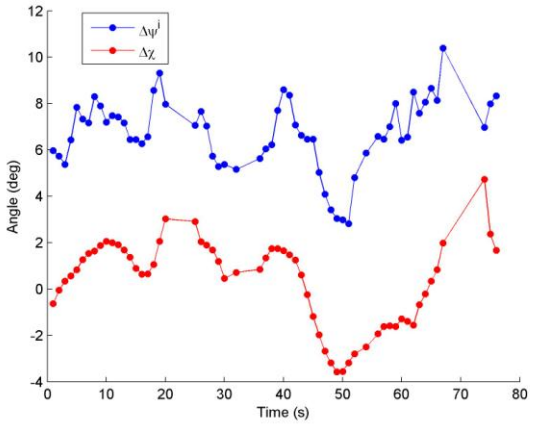


*Fig. 6: Relative heading angle to threat from image and relative track angle to threat in navigation frame.*

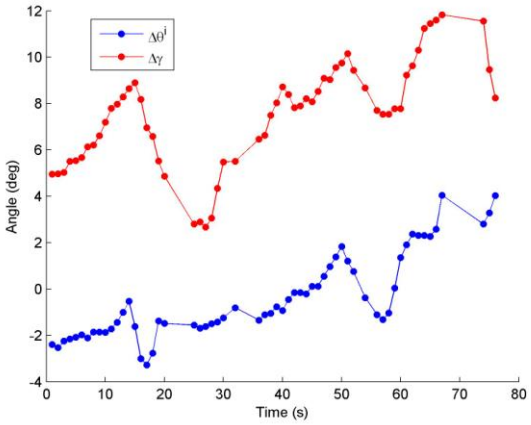


*Fig. 7: Relative pitch angle to threat from image and relative flight path angle to threat in navigation frame.*

Table I summarizes the difference between image-derived angles and true angles, averaged over the five test flights. A calculated average of 3 deg and 7.4 deg error for $\Delta\psi^i - \Delta\chi$ and $\Delta\theta^i - \Delta\gamma$ indicates that the errors in camera modelling (less than 1 deg from laboratory testing) were dominated by camera mounting misalignment and an unaccounted difference between body and navigation frame angles.

To examine the difference between body and navigation frame angles, the relative track and flight path angles $\Delta\chi^i$ and $\Delta\gamma^i$ were calculated from (3) and the angle errors $\Delta\chi^i - \Delta\chi$ and $\Delta\gamma^i - \Delta\gamma$ were calculated to be an average of 2.5 deg and 4.4 deg. These are 17% and 41% smaller than angles $\Delta\psi^i$ and $\Delta\theta^i$, which highlights that the difference between body and navigation frame angles can be significant and should be accounted for. We expect that the remaining errors included camera modelling, misalignment and other uncorrected effects (such as structural motion) and that these could be minimized further by a calibration process.

*Table 1: Errors between image-derived angles and true angles (averaged over 5 collision scenario flights).*

| | min (°) | max (°) | avg (°) |
|---|---|---|---|
| $\lvert\Delta\psi^i - \Delta\psi\rvert$ | 1.5 | 3.5 | 2.5 |
| $\lvert\Delta\theta^i - \Delta\theta\rvert$ | 10.0 | 11.1 | 10.5 |
| $\lvert\Delta\psi^i - \Delta\chi\rvert$ | 1.0 | 5.5 | 3.0 |
| $\lvert\Delta\theta^i - \Delta\gamma\rvert$ | 4.2 | 9.4 | 7.4 |
| $\lvert\Delta\chi^i - \Delta\chi\rvert$ | 1.6 | 3.4 | 2.5 |
| $\lvert\Delta\gamma^i - \Delta\gamma\rvert$ | 0.3 | 8.2 | 4.4 |

## Test Case 2: Impact of Angle Measurement Errors on Minimum Range to Threat

This test examined the impact of angle measurement errors on the achievable minimum range to a threat by simulation of a closed-loop lateral collision avoidance control scenario in MATLAB. Two aircraft (ownship and an intruder threat) were approximated by simplified aircraft dynamics (1) and set on a head-on collision course with straight line trajectories at constant speed. Ownship included a simulated camera model with a detection range of 1900 m and field of view of 60 deg. The simulated camera model was coupled with the avoidance control strategy described previously (Fig. 2) to change course when the threat aircraft came within range and field of view of the camera (see Fig. 8). Only the horizontal manoeuvre avoidance performance was assessed.

Ownship was travelling at constant 51 m/s and the tests were repeated for a range of initial relative bearing angles to the intruder aircraft (from -30 to 30 deg), and range of intruder constant flight speeds $V_i$ from 0 m/s (e.g. a balloon) to 110 m/s (e.g. a fast light aircraft). Increasing angle-from-image measurement biases were applied and the minimum range to the threat was recorded. Results are shown for 0 deg, 2 deg, 5 deg and 10 deg of bias on Fig. 9-12. It is observed that for an angle bias error of 5 deg or greater (Fig. 11, 12) the minimum range characteristics appear significantly different than for an angle bias of 5 deg or less (Fig. 9, 10).

The control policy resulted in a symmetrical and near-linear characteristic between relative bearing and minimum range (Fig. 9), and out of all the flight speeds the 0 m/s case typically had smallest minimum range. Knowledge of these characteristics could allow prediction of expected achievable minimum ranges to a threat. However, an increasing angle bias violated the control policy, resulting in non-linear and asymmetrical characteristics (Fig. 11, 12). As bias increased, it was more difficult to predict minimum ranging performance of the system. Also, increasing bias resulted in overly conservative manoeuvres (minimum range is up to 900 m for a bearing angle of 30 deg in Fig. 11 and 12, compared with 450 m for Fig. 9 and 10). Fortunately, despite the presence of large biases causing violation of the desired control policy, a collision never resulted (minimum range was always > 200 m), highlighting the effectiveness of the control avoidance approach in this collision scenario.

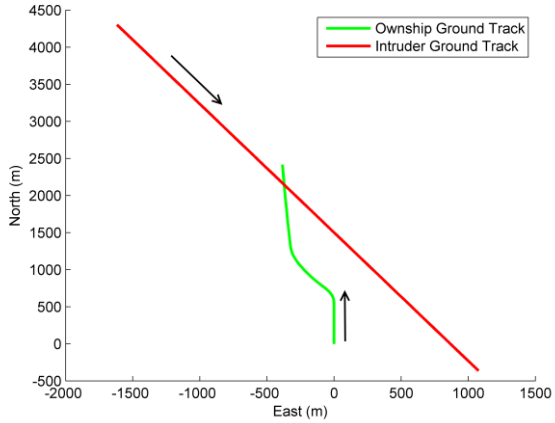


*Fig. 8: Ground track for collision avoidance scenario. The ownship successfully avoided a pending collision by detecting the intruder and keeping it at a fixed position in the image until the intruder left the image and passed by.*

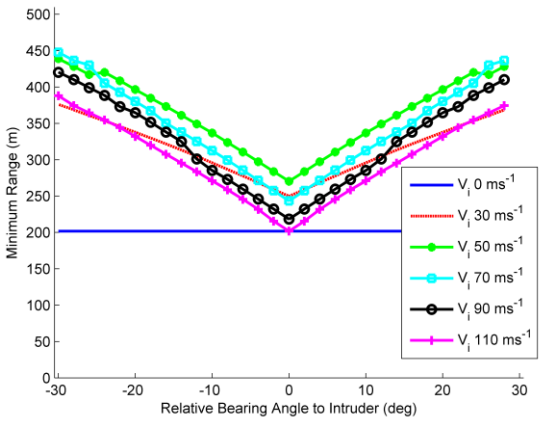


*Fig. 9: The effect of 0 deg angle bias on minimum range for different initial relative bearing angles and speeds.*

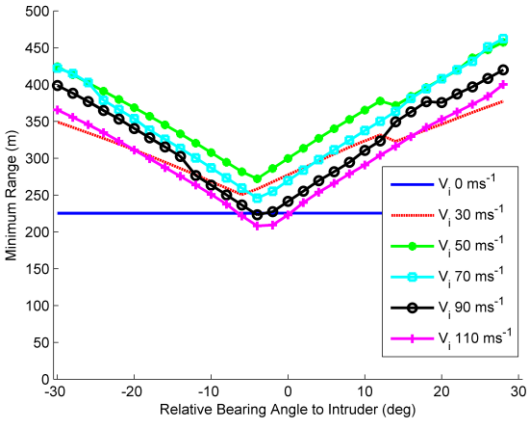


*Fig. 10: The effect of 2 deg angle bias on minimum range for different initial relative bearing angles and speeds.*

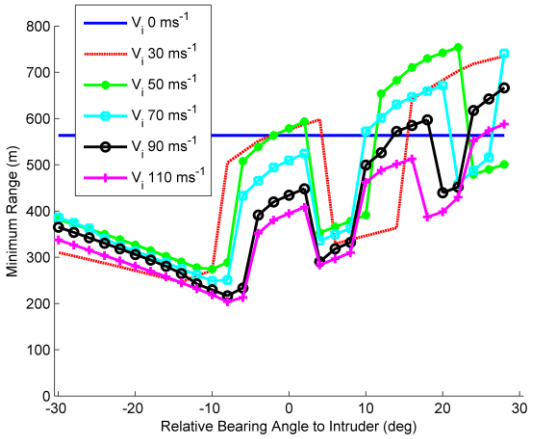


*Fig. 11: The effect of 5 deg angle bias on minimum range for different initial relative bearing angles and speeds.*

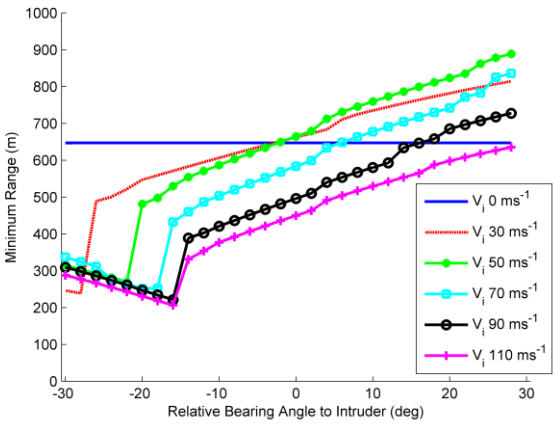


*Fig. 12: The effect of 10 deg angle bias on minimum range for different initial relative bearing angles and speeds.*

## Conclusion

Collision scenario flight tests with two light aircraft have provided useful real-world accuracy measurements of image-derived angles to a threat for use in vision-based collision avoidance. The flight tests indicated that camera mounting misalignment as well as unaccounted drift and attack angles were the dominant errors on the image-derived angle measurements. These results were used in a simulation study to assess the performance of vision-based reactive and passive collision avoidance under presence of angle measurement errors to the threat. Vision-based avoidance control simulations showed that angle bias errors greater than 5 deg had significant effect on the minimum range to threat characteristics. This would make estimation of safety margins difficult when only image information is available (no ranging). However an angle bias never resulted in a collision in these studies (minimum range was always greater than 200 m), highlighting the effectiveness of the collision avoidance approach. This investigation is part of a broader program which will soon demonstrate a complete and autonomous electro-optical based collision avoidance system for manned and unmanned vehicles.

## Acknowledgements

This research was supported under Australian Research Council's Linkage Projects funding scheme (project number LP100100302) and the Smart Skies Project, which is funded, in part, by the Queensland State Government Smart State Funding Scheme. The authors would like to acknowledge all test pilots, engineers and researchers Rhys Mudford, Duncan Greer, Felipe Gonzalez, Scott McNamara, Chris Turner, Richard Glassock, Reece Clothier and John S. Lai for their involvement in the reported flight tests and the construction of the specialised equipment.

## References

1. G. Ambrosino, M. Ariola, U. Ciniglio, F. Corraro, E. De Lellis, and A. Pironti. Path generation and tracking in 3-d for uavs. IEEE Transactions on Control Systems Technology, 17(4), 2009.

2. Pascual Campoy, Juan F. Correa, Ivan Mondragón, Carol Martínez, Miguel Olivares, Luis Mejías, and Jorge Artieda. Computer vision onboard UAVs for civilian tasks. Journal of Intelligent Robotic Systems, 52(3):1–31, 2008.

3. Su-Cheol Han, Hyochoong Bang, and Chang- Sun Yoo. Proportional navigation-based collision avoidance for UAVs. International Journal of Control, Automation, and Systems, 7(4):553– 565, 2009.

4. M. Kayton and W.R. Fried. Avionics Navigation Systems. JohnWiley and Sons, 2nd edition, 1997.

5. J. Lai, L. Mejias, and J.J. Ford. Airborne vision-based collision-detection system. Journal of Field Robotics, 28(2):137–157, 2010.

6. Aaron Mcfadyen, Luis Mejias, and Peter Corke. Visual servoing approach to collision avoidance for aircraft. In 28th Congress of the International Council of the Aeronautical Sciences, 2012.

7. Luis Mejias, Jason Ford, and John Lai. Towards the implementation of vision-based UAS sense and- avoid. In Proceedings of the 27th International Congress of the Aeronautical Sciences (ICAS 2010 CD-Rom), 2010.

8. Jung-Woo Park, Hyon-Dong Oh, and Min-Jea Tahk. UAV collision avoidance based on geometric approach. In SICE Annual Conference 2008, Japan, 2008.

9. B. L. Stevens and F. L. Lewis. Aircraft control and simulation. Wiley-Interscience, Georgia Tech Research Institute/University of Texas, 1992.

10. S. Temizer, M.J. Kochenderfer, L.P. Kaelbling, T. Lozano-Perez, and J.K. Kuchar. Collision avoidance for unmanned aircraft using Markov decision processes. In AIAA Guidance, Navigation, and Control Conference, Toronto, Canada (2010), 2010.

11. X. Yang, L. M. Alvarez and T. Bruggemann, A 3D Collision Avoidance Strategy for UAVs in a Non-Cooperative Environment, Journal of Intelligent and Robotic Systems, 12 Aug 2012, DOI:10.1007/s10846-012-9754-x

12. Saunders, J., Beard, R.: Reactive vision-based obstacle avoidance with camera field of view constraints. In: AIAA Guidance, Navigation and Control Conference and Exhibit. Honolulu, Hawaii (2008)

13. K.N. Boyadzhiev, Spirals and conchospirals in the flight of insects. Coll. Math. J. 30(1), 23–31 (1999)